# Microbial carbon use for incorporating biomass phosphorus drives $CO_2$ emission in phosphorus-supplied subtropical forest soils

Jianghao Tan [1,3#], Muhammed Mustapha Ibrahim [1#], Huiying Lin [1,2], Zhaofeng Chang [1,2], Conghui Guo [1,2], Zhimin Li [1], Xianzhen Luo [1], Yongbiao Lin [1], Enqing Hou [1*]

[1] Guangdong Provincial Key Laboratory of Applied Botany & Key Laboratory of National Forestry and Grassland Administration on Plant Conservation and Utilization in Southern China, South China Botanical Garden, Chinese Academy of Sciences, Guangzhou 510650, China

[2] University of Chinese Academy of Sciences, 100039, Beijing, China

[3] Shanxi Agricultural University, Jinzhong 030801, China

[#] These authors contributed equally to this work

* Corresponding author: houeq@scbg.ac.cn (E. Hou).

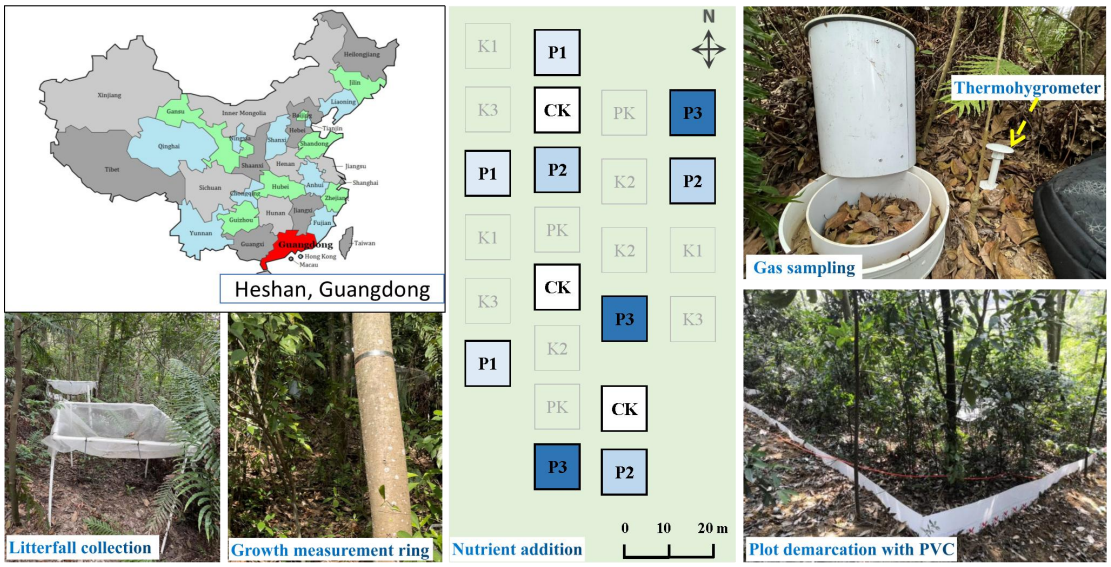


**Fig. S1.** Study site showing phosphorus and potassium addition in an evergreen broad-leaved forest at the station (Note: only four phosphorus addition treatments were used in the current study: +0, +25, +50, and +100 kg P $ha^{-1}$ $yr^{-1}$, and three replicates of each treatment were denoted by CK, P1, P2, and P3, respectively)

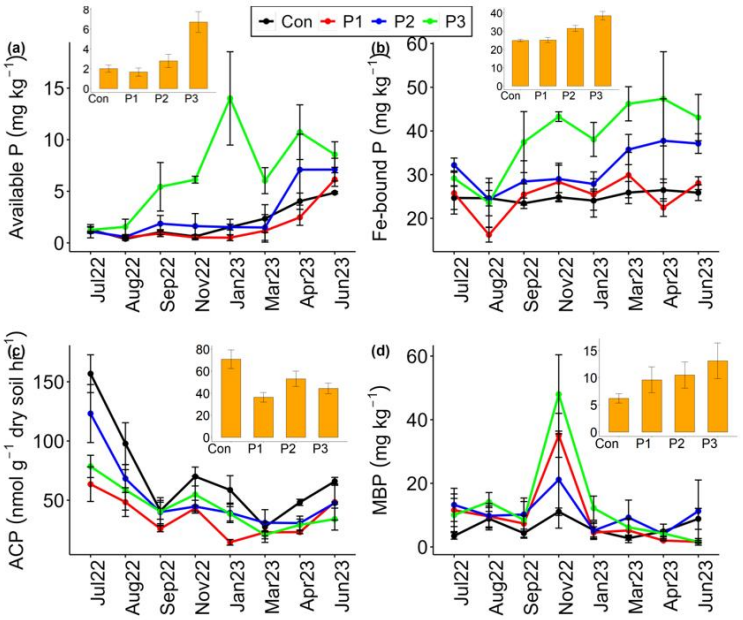


**Fig. S2.** Repeated measures of soil P dynamics over one year after phosphorus (P) additions in the 10-20 cm depth. (a) available P concentration extracted by Bray-1 method, (b) iron-bound P (NaOH Pi) concentration, (c) acid phosphatase activity, and (d) microbial biomass P concentration. Each line/bar represents the mean value of each treatment (n=3 (lines), n=24 (bars), $p < 0.05$). The error bars represent the standard error of the mean. Con: control, P1: 25 kg P $ha^{-1}$, P2: 50 kg P $ha^{-1}$, P3: 100 kg P $ha^{-1}$.

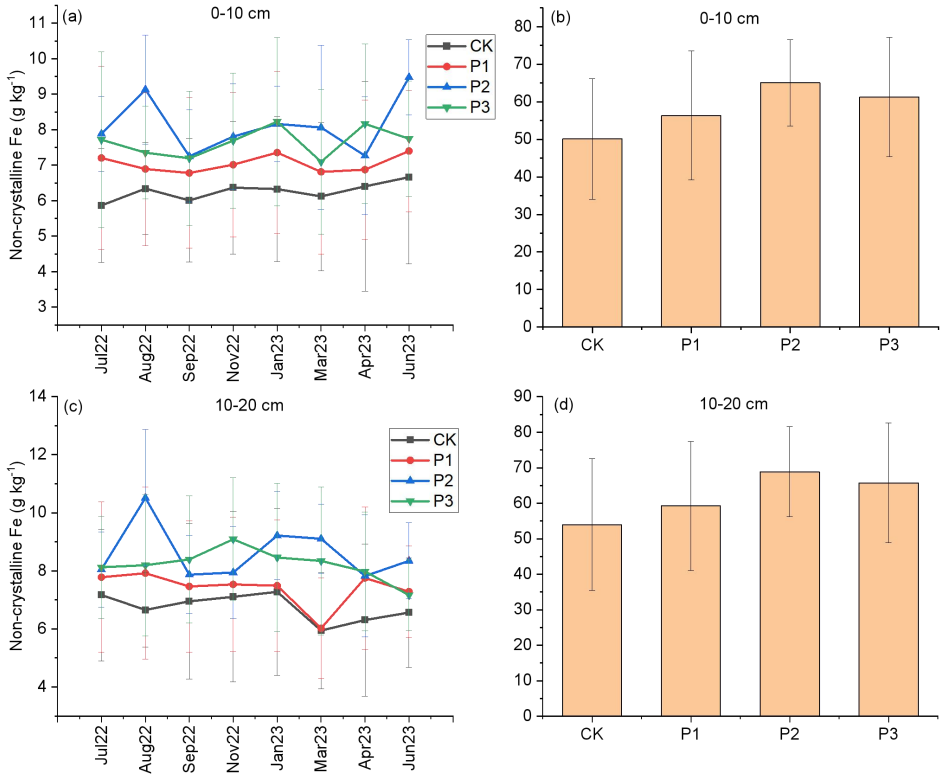


**Fig. S3.** Dynamics of non-crystalline iron (Fe) concentration across sampling times in different soil depths following P addition. a. non-crystalline Fe concentration across sampling time in the 0-10 cm depth, b. cumulative non-crystalline Fe concentration in the 0-10 cm depth, b. non-crystalline Fe concentration across sampling time in the 10-20 cm depth, and d. cumulative non-crystalline Fe concentration in the 10-20 cm depth. Each line/bar represents the mean value of each treatment (n=3 (lines), n=24 (bars), $p < 0.05$). The error bars represent the standard deviation of the mean, using Tukey's test (n=24, $p < 0.05$). CK: control, P1: 25 kg P ha$^{-1}$, P2: 50 kg P ha$^{-1}$, P3: 100 kg P ha$^{-1}$.

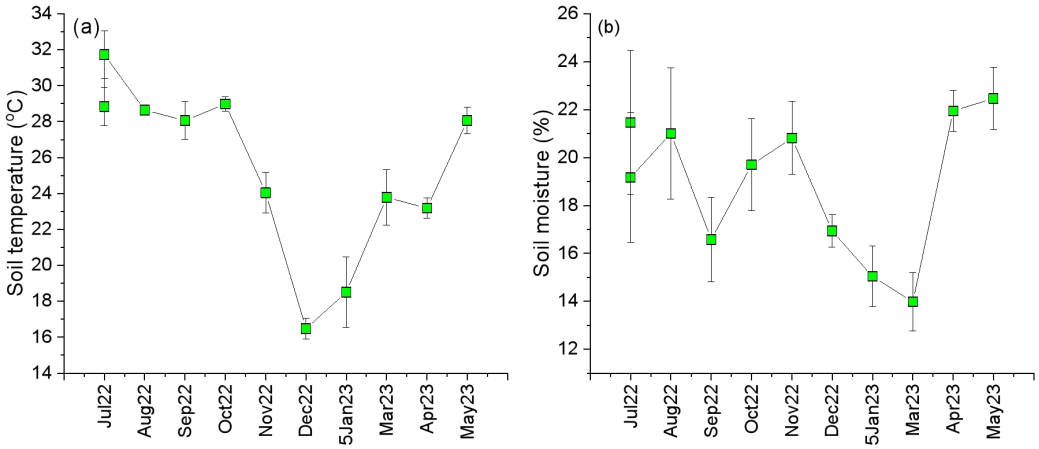


**Fig. S4.** Dynamics of soil physical properties a. soil temperature, and b. soil moisture content. Each line/bar represents the mean value of each treatment (n=6 $p < 0.05$). The error bars represent the standard error (SE) of the mean, using Tukey's test

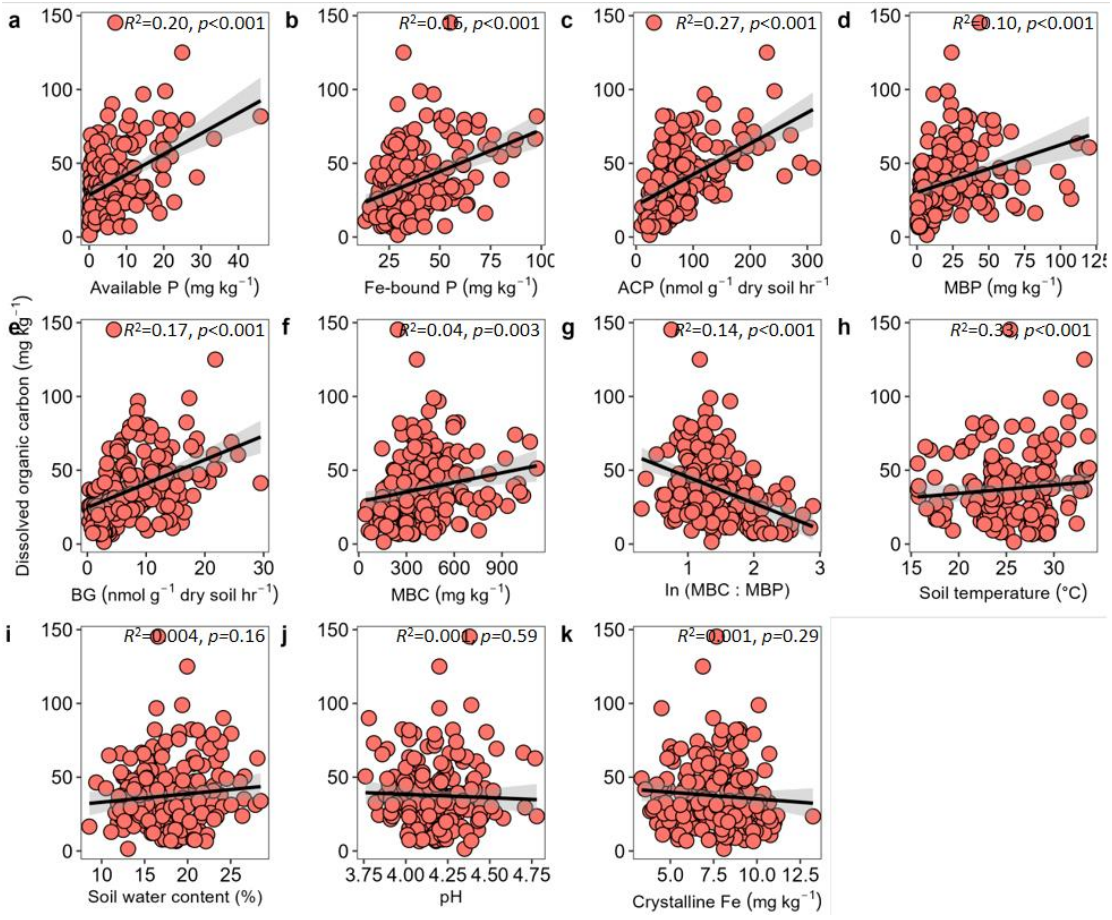


**Fig. S5.** Linear regression modeling showing the relationships between dissolved organic carbon (C) and soil phosphorus (P) and C fractions in the 0-20 cm depth following P supplies. ACP: acid phosphatase, BG: beta-glucosidase, MBC: microbial biomass C, MBP: microbial biomass P, Fe: iron

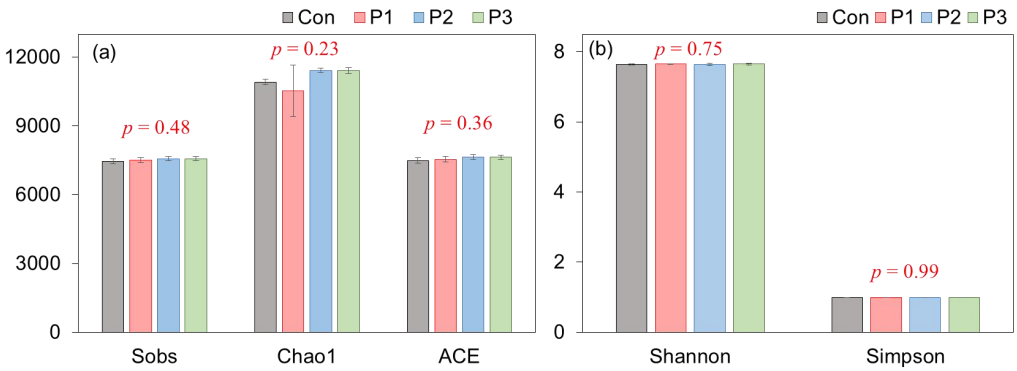


**Fig. S6.** Alpha diversity indices of total microbial gene knockout identities following phosphorus addition. a. Observed Species (Sobs), Chao1, and Abundance-based Coverage Estimator (ACE) and b. Shannon and Simpson indices. Con: control, P1: 25 kg P $ha^{-1}$, P2: 50 kg P $ha^{-1}$, P3: 100 kg P $ha^{-1}$.

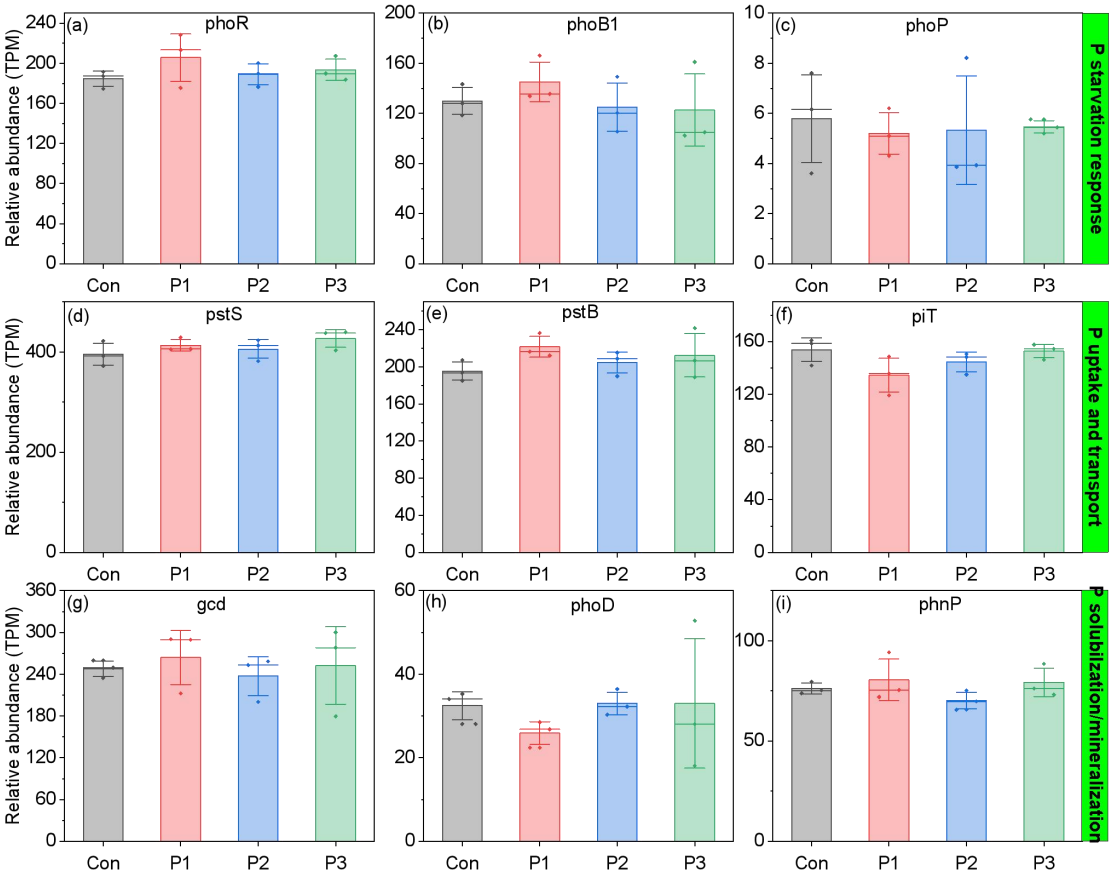


**Fig. S7.** Shifts in the relative abundance of phosphorus cycling functional gene knockouts following P addition. TPM: transcripts per million, CK: control, P1: 25 kg P $ha^{-1}$, P2: 50 kg P $ha^{-1}$, P3: 100 kg P $ha^{-1}$.